

Landslide Susceptibility Assessment Using GIS-Based Weights-of-Evidence Model in the Khimti Khola Watershed, Eastern Nepal

Milan Kumar Rai^{1*} Surendra Maharjan² and Ranjan Kumar Dahal³

1. Central Department of Geology, Tribhuvan University, Kirtipur, Nepal

2. Department of Civil Engineering, Pulchowk Campus, IoE, TU, Nepal

3. Central Department of Geology, Tribhuvan University, Kirtipur, Nepal

ABSTRACT

The Khimti Khola watershed of the Eastern Nepal experiences numerous landslides each year, pose a significant natural hazard that can cause property damage and fatalities. In mountainous areas like Nepal, an accurate evaluation of landslide hazards may be an essential tool for disaster risk reduction and the strategic planning of development initiatives. To address this concern, a landslide susceptibility assessment was conducted in the Khimti Khola watershed, which covers an area of 440 km². The purpose of this assessment is to locate areas that are susceptible to landslides and to provide light on the factors that affect them. A total of 415 landslides were identified, covering 1.715 km² or 0.39% of the entire study area. The assessment derived the landslide susceptibility map using the Weights-of-Evidence (WoE) model from selected conditioning factor classes that were processed in ArcGIS and categorized into five classes: Very High, High, Moderate, Low, and Very Low. Each of these classes covers 7.12%, 16.63%, 25.23%, 30.24%, and 20.78% of the total study area, respectively. According to the findings, the Khimti Khola watershed has a 33.2% landslide occurrence percentage in the high susceptibility zone, out of the total area. Additionally, the very high, moderate, low, and very low susceptibility zones cover 24.35%, 20.75%, 17.08%, and 4.62% area of the landslide occurrence, respectively. In this assessment, the Area Under Curve (AUC) is used to validate the model and is plotted using ArcSDM. Identified a total of 415 landslides, out of which 311 (75%) were used as training sample for susceptibility mapping, while the remaining 104 (25%) were used to validate. The AUC for the landslide susceptibility map is 83%, indicating a very good degree of accuracy and satisfaction. The resulting susceptibility map provides information for predicting landslide-prone areas. It can be used to minimize the risk of potential landslides, safeguard lives, and prevent property damage. It will be a vital tool for disaster preparedness, future construction planning and development projects in this area.

Keywords: Landslides, Weights-of-Evidence Model, Landslide Susceptibility Assessment, Khimti Khola Watershed, Eastern Nepal.

Received : 13 July 2022

Accepted : 10 December 2022

INTRODUCTION

The mountainous terrain of the Nepal Himalaya exhibits a remarkably dynamic and fragile mountain landscapes. Every year, Nepal experiences numerous landslides, which are influenced by factors such as intense weathering, climate change, unpredictable hydrology, and human interventions like the development of road networks and other infrastructure. The Himalayas stand as a highly fragile mountain range, primarily owing to the inherent geological fragility of their rocks and soils (Upreti, 2001). The frequency and impact of landslides have grown due to population growth and the construction of road networks, infrastructure, communities, and lifelines (Guzzetti, 2005).

In Khimti watershed region, many hydropower projects lie, some are being under construction, also the Feasibility Study and Environmental Impact

Assessment (EIA) Study of Khimti Those Siwalaya Storage Hydropower project is conducting by the Department of Electricity Development (DoED), which is one of the largest storage capacity reservoir projects in Nepal. This region is vulnerable to landslides (Thakurathi et al., 2021) thus it is necessary to assess the vulnerability of this area.

Normally, a landslide susceptibility index (LSI) is used to perform landslide susceptibility mapping, which is determined through various approaches: Deterministic (Dai et al., 2002, Chimidi et al. 2017, Girma et al. 2015); Heuristic approach (Van Westen et al., 2000); and Statistical method (Van Westen, 1993). The deterministic approach uses appropriated mathematical models to calculate the safety factor for unstable slopes. Its primary emphasis is on hydrological and geotechnical characteristics evaluation of unstable soil and rock formations (Regmi et al., 2014a). According to Regmi et al. (2014a), a heuristic approach is a

Direct as well as indirect mapping that determines

*Corresponding author's
email: egeologistmilan@gmail.com (M.K. Rai)

the relationship between the causes of slope failures and their occurrence. Statistical techniques include statistical study of the geographical distribution of landslides and the many factors that contribute to their occurrence to determine the connection between topographical factors and the occurrence of landslides (Lee and Choi, 2004). Bivariate and multivariate approaches are frequently used statistical methods for the susceptibility mapping of landslides. The bivariate approach compares the landslide inventory map with the factor maps to assign weights and by superimposing these factor maps, susceptibility map of landslides was created. Frequency ratio (Thakurathi et al., 2021), Weights-of-Evidence (Dahal et al., 2008, Mohammady et al., 2012, Gadtula and Dhakal, 2019; Batar et al., 2021, Cao et al., 2021, KC et al., 2022, Dam et al., 2022, Mandal et al., 2023) and certainty factor are some of the bivariate statistical methods (Devkota et al., 2013, Pradhan and Lee, 2010) and the multivariate methods include logical regression, discriminant analysis, and decision trees (Kavzoglu et al., 2015). Similarly other methods are artificial neural networks (ANNs), fuzzy logic, support vector machine, neuro-fuzzy model (Pradhan, 2010). Several methodologies have been developed for assessing landslide hazards, ranging from empirical models to advanced statistical approaches. Among these methodologies, the GIS-based Weight of Evidence method is applied to develop the landslide susceptibility map in this assessment. A

combination of aerial photos, satellite photos and images, Geographic Information Systems (GIS), remote sensing data and on-site field observations are used to create an inventory map of landslides and then analyze the factors. The model is validated in this assessment using the Area Under curve (AUC). ArcSDM, a tool for Receiver Operating Characteristics (ROC) analysis of spatial models for GIS, is used to create the graph (Mas J-F et al., 2013). The assessment provides valuable insights into landslide hazard assessment and can be used as a reference for future research in other regions with similar characteristics.

STUDY AREA

The research area belongs to the Khimti Khola Watershed of Eastern Nepal, which is a major river system spanning bordered two districts, Dolakha and Ramechhap (Fig.1). The area of the watershed is around 440 km². The Khimti Khola begins from the southern slope of the Rolwaling Himalayan range and flows southward before joining the Tamakoshi River which is the major river in the Koshi Basin. The watershed is characterized by steep slopes, rugged terrain, and high precipitation, with an average annual rainfall of 1600-2500 mm. The elevation above mean sea level (masl) varies from 548 to 5406 meters.

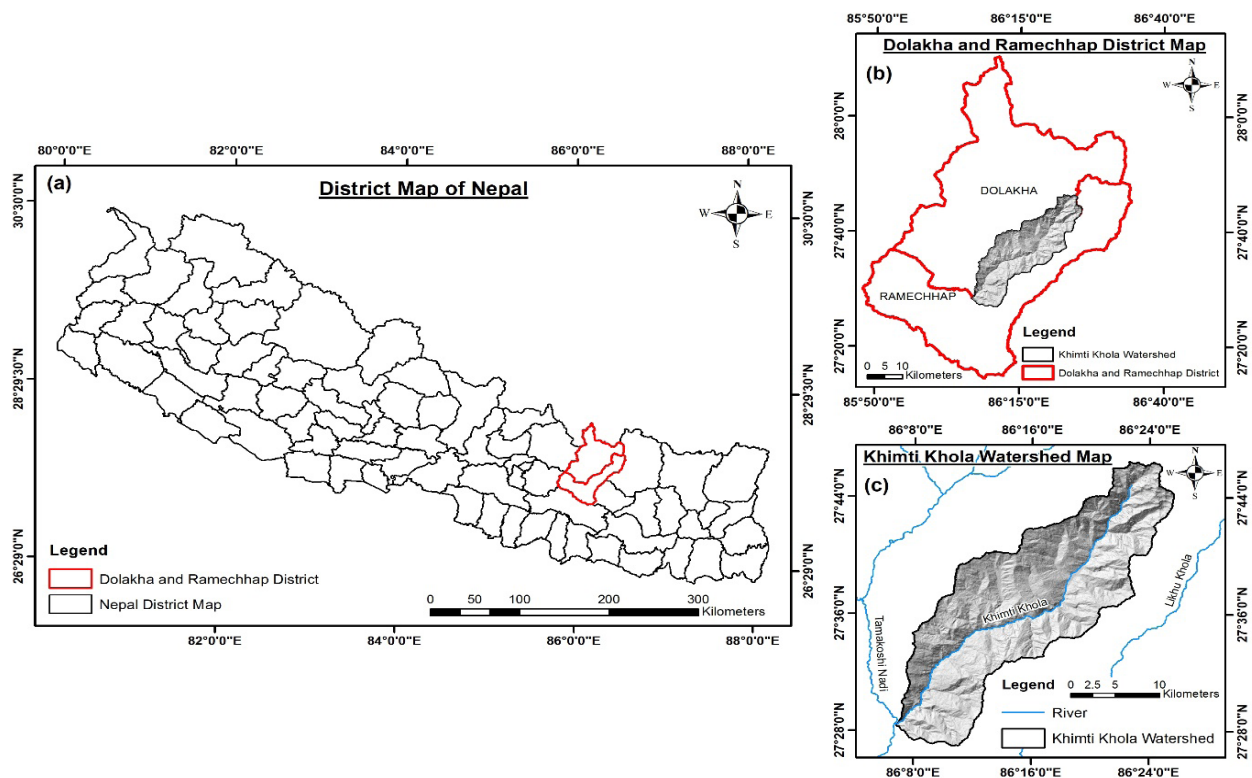


Fig.1: Location map (study area) (a) Dolakha and Ramechhap districts in Nepal. (b) Study area location (Khimti Khola watershed) in Dolakha & Ramechhap districts. (c) The Khimti Khola Watershed and other major rivers.

Due to its geological setting, topography, and climatic conditions, the area is prone to landslides. Khimti Khola watershed is susceptible to the landslide susceptibility and also data of that region is available so this area was chosen for this study.

ASSESSMENT METHOD

The geographic information relevant to our research area was obtained from pre-existing databases to simplify the numerical evaluation of the susceptibility to landslides. This research delved into twelve primary factors commonly associated with landslide occurrences on a field scale. These factors include Slope, Elevation, Curvature, Aspect, Topographic Wetness Index (TWI), Standardized Precipitation Index (SPI), Distance from streams, Landuse/Landcover, Lithology, Distance from Thrust/Fault lines, Rainfall Patterns, and Distance from Roads. Each of these variables was carefully considered in our efforts towards landslide susceptibility mapping.

Data Acquisition and Processing

The high-resolution terrain-corrected ALOS PALSAR Digital Elevation Model (DEM), accessible through the Alaska Satellite Facility website (<https://asf.alaska.edu>), was acquired and processed for the current analysis. This DEM boasts a resolution of 12.5 meters by 12.5 meters per pixel. Utilizing the ALOS PALSAR DEM, thematic data

layers such as elevation, slope, aspect, curvature, standardized precipitation index (SPI), and topographic wetness index (TWI) were derived. These layers were meticulously prepared using ArcGIS 10.8 (ESRI, USA) to cover the entirety of the area.

The lithology map was compiled using references from the Geological Map of Eastern Nepal (Shrestha et al., 1984), data from the Department of Mines and Geology (DMG) and supplemented by field investigations. For the land use/land cover (LULC) map, data were extracted from the ICIMOD regional database system. All thematic data pertaining to causative factors were readily discerned within the GIS tool. These data were derived and analyzed based on the Digital Elevation Model (DEM) using the Weight-of-Evidence (WoE) model, as illustrated in Fig.2, to facilitate susceptibility assessment.

Landslide Susceptibility Modeling

The Weights-of-Evidence (WoE) model represents a loglinear adaptation of the Bayesian probability model, employing a bivariate statistical approach to ascertain the relative weight of evidence. The foundational work by Bonham-Carter et al. in 1989 provides an in-depth mathematical framework for the WoE methodology. For every factor considered, as every pixel or point on the map represents a specific class F, the weights for its presence (W+) and absence (W-) of this particular class can be computed as described below.

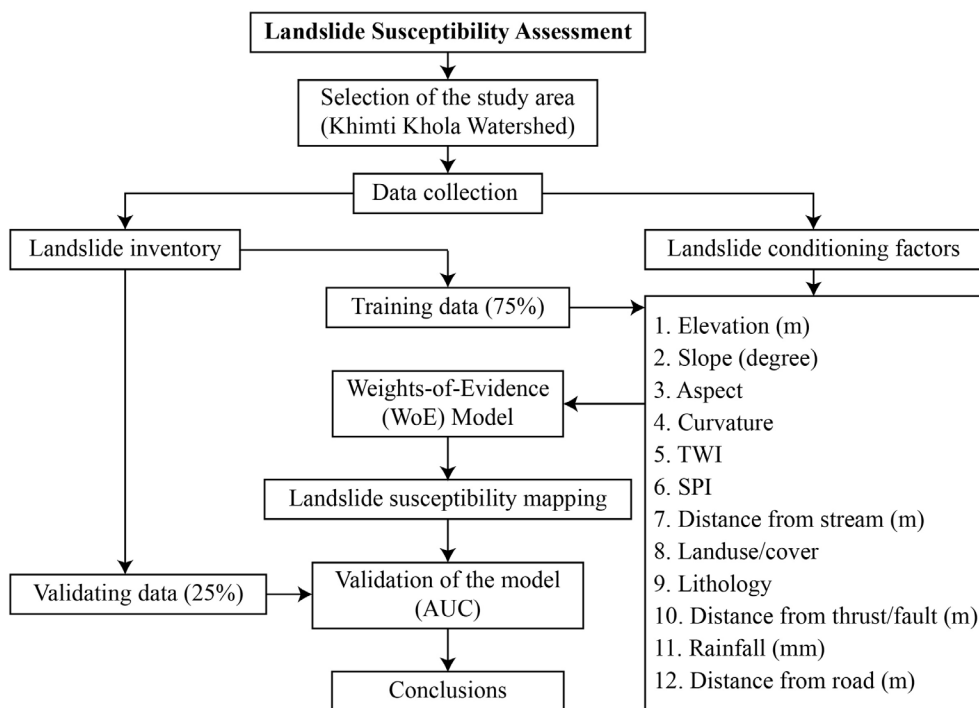


Fig.2: Landslide Susceptibility Assessment by using Weights-of-Evidence (WoE) Model.

$$W^+ = \ln \frac{P(F|L)}{P(F|\bar{L})} \quad (1)$$

$$W^- = \ln \frac{P(\bar{F}|L)}{P(\bar{F}|\bar{L})} \quad (2)$$

In the equations provided above and in subsequent equations, the variable P denotes probability. The Letter L signifies that the landslides are present, using a similar method. Here, $P(\bar{F}|L)$ denotes the while L the landslides are absent; Similarly F and probability of class F being absent in the presence signifies the specific class pertaining to a given factor. As a result, $P(F|L)$ indicates the probability of particular class under the presence of a landslide, and $P(F|\bar{L})$ Indicates the probability of the specific class in the absence of landslides. These probabilities can be readily calculated from the pixel values within the distribution map. $P(F|L) = N(F|L)/N(L)$; $N(F|L)$ is the probability of class F given the presence of landslides, and $N(L)$

represents the total number of pixels of landslides in class F. Likewise, it can be demonstrated that $P(F|\bar{L}) = N(F|\bar{L})/N(\bar{L})$, $N(F|\bar{L})$ represents the number of pixels of non-landslide in class F and $N(\bar{L})$ denotes the total number of non-landslide pixels on the map.

The weight for a specific class which is absent, denoted as, W, in Equation (2), can be determined of landslides, and $P(\bar{F}|L)$ indicates the likelihood of class F being absent in the absence of landslides.

Calculating both probabilities is straightforward; $P(\bar{F}|L) = N(\bar{F}|L)/N(L)$; $N(\bar{F}|L)$ represents the number of pixels of landslides in all classes other than F.

Similarly, $P(F|\bar{L}) = N(F|\bar{L})/N(\bar{L})$, $N(\bar{F}|\bar{L})$ denotes the count of pixels representing non-landslide instances across all classes except F. The weight contrast, denoted as C, signifies the disparity between these two weights.

$$C = W^+ - W^- \quad (3)$$

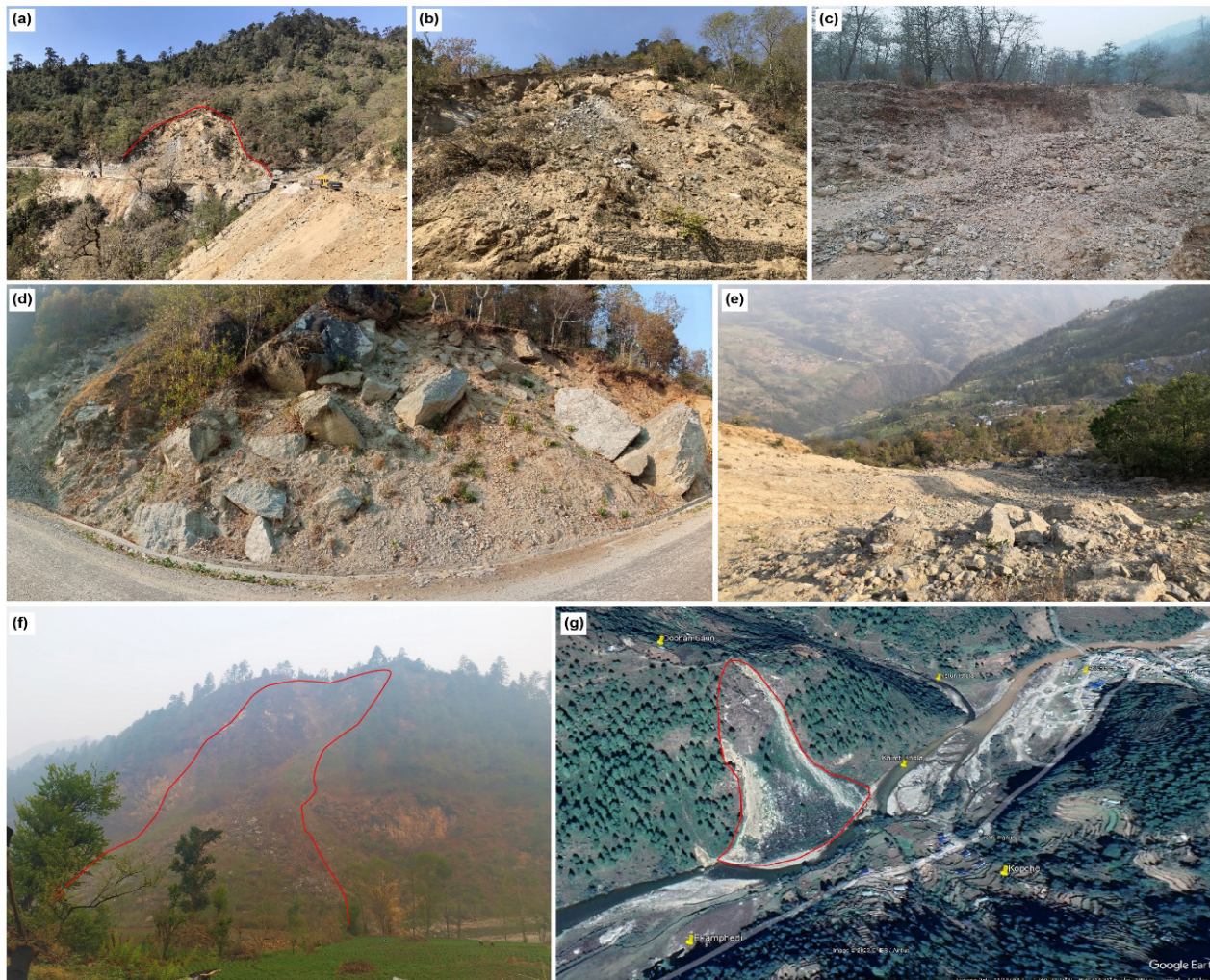


Fig.3: Several photographs showing the landslides that have been observed in the Khimti Khola Watershed: (a) and (b) Landslides triggered by excavation activities, characterized by multiple scarps along the Khawa-Jiri Road Section. (c) Debris flows (d) and (e) Landslides induced by excavation activities, displaying multiple scarps along the Hawa-Jiri Road Section in the vicinity of Chyama. (e) Ekamphedi landslide, and (f) Google Earth image shows the Ekamphedi landslide located downstream from the confluence of Yelun Khola and Khimti Khola of the Shivalaya area.

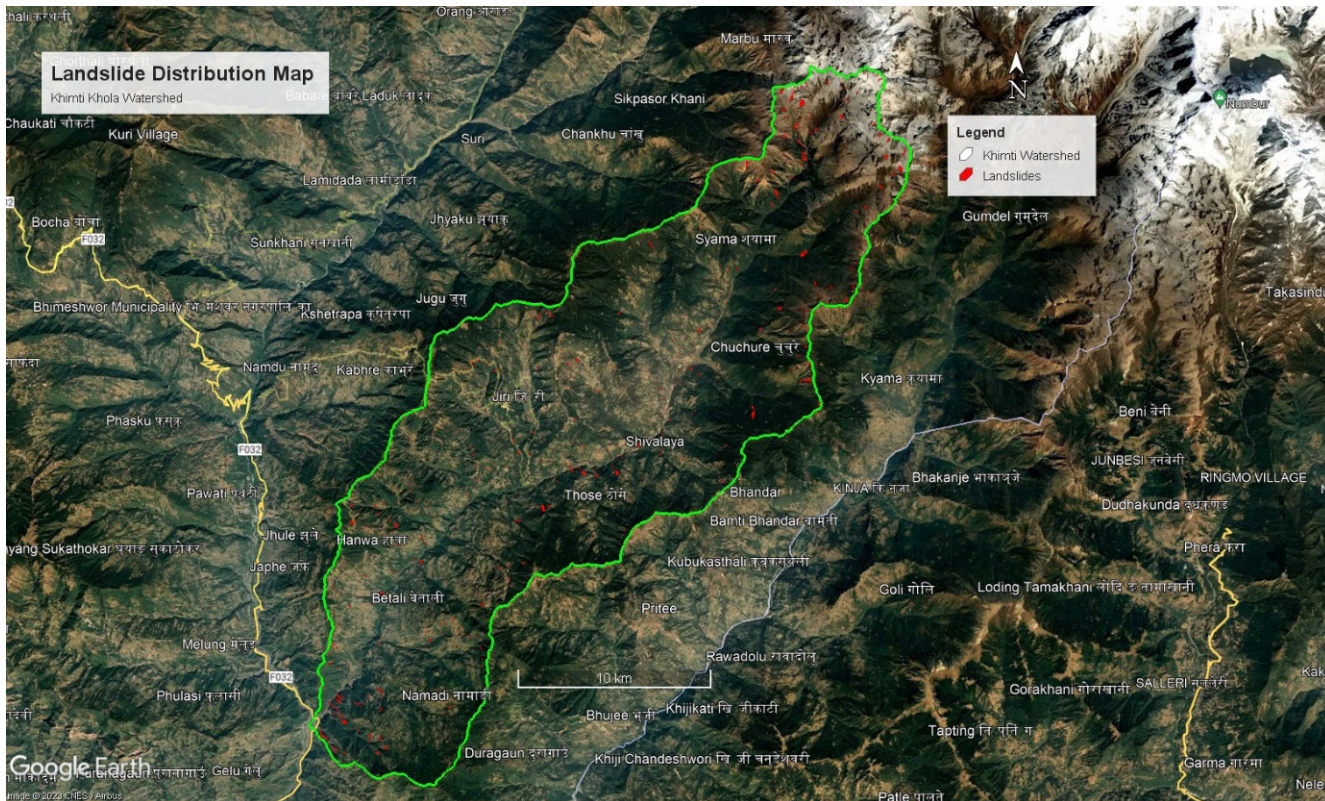


Fig.4: Google imagery view of Landslides distribution at the study area.

The overall spatial correlation between the landslides and the particular class of the factor is reflected in the magnitude of contrast. A negative value implies the absence of spatial association, whereas a positive value indicates the presence of spatial association. According to Neuhäuser and Terhorst, 2007; typically normalize this number by dividing C by its standard deviation, represented as $S(C)$. The result obtained is a value of $C/S(C)$, which acts as a quantitative indicator of the spatial correlation's importance.

LANDSLIDE INVENTORY MAP

Khimti Khola watershed was selected for study area based on its susceptibility to landslides. The landslide inventory map and conditioning factor analysis were conducted using a combination of satellite imagery, aerial images, Geographic Information Systems (GIS), and on-site observations. The assessment identified 415 landslides within the study area, encompassing an area of 1.715 Km², equivalent to 0.39% of the total study area. These landslides predominantly occurred in regions characterized by steep slopes, high precipitation levels, recent road construction activities and sparse vegetation cover. Different landslides were identified, including the reactivation of old landslides, colluvium deposits, gully erosion, debris slides, rock slides, rock falls, road cut slides, and slope failures.

LANDSLIDE CONDITIONING FACTORS

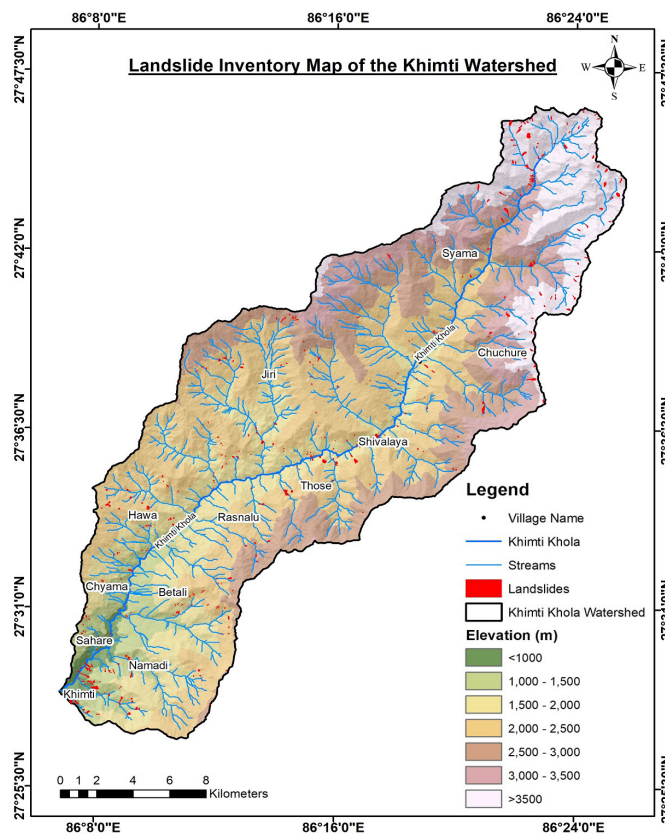


Fig.5: Map depicting the study area and the inventory of landslides present on that area; each region highlighted by red polygons indicates the location of a landslide.

Twelve landslide conditioning aspects that are critical for this landslide susceptibility assessment have been taken into consideration. Using the WoE technique, the spatial connection between each conditioning factor for landslides and actual landslide occurrences has been summarized and presented in Table 1. These factors and their distributions are described as follows:

Elevation

Pachauri and Pant (1992) reported landslides are more likely to occur in places of higher elevation and are more susceptible to occur in areas with higher relief (Ercanoglu et al., 2004). In employing the WoE approach, the elevation factor is utilized to assess the association between elevation and landslide occurrences. The distribution of landslides in the elevation map of the study area is shown in Fig. 6a. The elevation map has been categorized into 7 distinct classes: <1000 m, 1000 - 1500 m, 1500 - 2000 m, 2000 - 2500 m, 2500 - 3000 m, 3000 - 3500 m, and >3500 m. The most significant positive weight contrast was observed in the >3500 m zone.

Slope

Slope plays a significant role in assessing a property's susceptibility to landslides because steep slopes are more prone to produce landslides. The landslide distribution of the slope map is shown in Fig. 6b. The slope map has been categorized into 5 classes: <15 degrees, 15-30 degrees, 30-45 degrees, 45-60 degrees and >60 degrees. Evidently, the slope angle of 30 - 45 degree has high weight contrast correlation with landslide.

Aspect

According to Lee et al. 2004, one of the important components in the development of landslide susceptibility map is the aspect. The aspect has a crucial role in landslides due to its impact on moisture and precipitation (Ghimire, M 2011). Physically, the aspect relates to factors including precipitation, wind impact, sun exposure, and the direction of discontinuities influencing landslides (Ercanoglu et al., 2004). Nine distinct classes have been assigned to the aspect map (Fig. 6c), including North, South, East, West, North East, South East, North West, South West and Flat. The analysis reveals that the southwest facing slope has high weight contrast correlation with landslides.

Curvature

Curvature influences the stability of slopes in rugged

terrain by either focusing or spreading surface and subsurface water, as discussed by Kayastha et al., 2012. The spatial pattern of landslides in the curvature map is shown in (Fig.6d) and has been divided into 3 different categories are concave, linear, and convex. The analysis reveals that the concave has high weight contrast correlation with landslide.

TWI

To assess the topographic influence on hydrological processes, TWI is often used. It is expressed by the following relationship (Beven and Kirkby, 1979)

$$TWI = \ln \frac{a}{\tan \beta}$$

where a = the total upslope area draining via a point and $\tan \beta$ = the slope angle at the location. The topographic wetness index has been divided into 4 categories; < 4, 4 - 6, 6 - 8, > 8 (Fig.7e).

SPI

The SPI measures the erosive force exerted by a stream on the slope, evaluating its ability to erode and its influence on stability. This index is determined by the relationship outlined by Moore and Grayson, 1991.

$$SPI = A \tan \beta$$

Here, A represents the flow accumulation area, and β denotes the specific slope gradient measured in degrees. The stream power index was divided into 4 categories: <100000, 100000-500000, 500000-1000000, and >1000000 (Fig. 7f).

Distance from stream

One significant contributing factor to the incidence of landslides is runoff. The closeness of nearby the local streams and rivers serves as a proxy for the distance from the stream. The distance from the stream refers to the distance between the point of interest and the nearest stream, which significantly influences the stability of the slope. Streams can adversely affect slope stability through toe-incision or by saturating the lower part of the hillslope material due to increasing water levels. The stability of a slope may also be significantly influenced by its saturation level. The map indicating distance from the stream has been categorized into 6 distinct classes: <100 m, 100 - 200 m, 200 - 300 m, 300 - 400 m, 400 - 500 m, and >500 m (Fig. 7g). This

indicates that distances less than 100 m exhibit a significant positive weight contrast, whereas distances between 400-500 m display a notably negative contrast correlation with landslides, suggests that landslides are more likely to occur at closer distances and decrease markedly with increasing distance from streams.

Landuse/cover

Slope stability is also greatly impacted by land cover and use. The forest cover stabilizes the hilly slope by holding the soil in place and preventing erosion. The ICIMOD, 2013 regional database system was used to create the land use/cover map of the research area (Fig. 7h). Six unique categories have been identified on the land use/cover map: forest, shrubland, grassland, agricultural area, barren area, and snow/glacier. The barren area and following grassland have the highest weight contrast correlation with landslides.

Lithology

lithology is a significant factor in landslide susceptibility assessment. Various geological units exhibit varying degrees of susceptibility to the dynamic geomorphological processes of the Himalayas. The characteristics of the lithology types and rock units play a vital role in the occurrence of landslides. Predominantly the study area lies in the Midland Schuppen zone of the Melung augen gneiss belongs to the Ulleri Formation of Lesser Himalayan sequence. The lithological map is prepared by the reference of the geological map of Eastern Nepal (Shrestha et al., 1984), DMG, and from field investigations as well. The lithology of study area is classified into nine different classes: Undifferentiated Hg, Himal Gneiss, Panglema Quartzite, Dware Kharka Schist, Ghanapokhara Formation, Seti Formation, Kushma Formation, Ulleri Formation and Naudada Formation. The main lithology types of the study area are gneiss, slate, schist, phyllite, and quartzite. The landslide distribution in the lithology map is shown in Fig.8i. It shows that the highest weight contrast is in the Undifferentiated Hg and following the Ulleri Formation.

Distance from thrust/fault

Landslides are commonly associated with tectonic fractures, such as faults and thrusts. The existence of fault/thrust lines at steep gradients creates favorable conditions for slope failure. MCT and some local fault lines are considered causal factors for slope instability in the study area. MCT and fault lines are generated from the geological map of Eastern

Nepal (MCT) and field investigations as well. Notably, the Main Central Thrust (MCT) passes in close proximity to the confluence of Yelun Khola and Khimti Khola in the Shivalaya area. Ekamphedi landslide in the Shivalaya area has been found to have a strong correlation with the MCT (Fig.3 f and g). The distance from the thrust map has been divided into 6 distinct categories: <100 m, 100 – 200 m, 200 – 300 m, 300 - 400 m, 400 – 500 m, and >500 m (Fig. 8j). It shows that distances > 500 m has a high weight contrast correlation with the occurrence of the landslide.

Rainfall

Rainfall impacts significantly to Himalayan landslides processes. According to Dahal et al. 2008, landslides in the Himalayas are more probable to occur when daily precipitation surpasses 144 mm. Landslides are more probable to occur as rainfall intensity increases. The WoE approach was used to examine the correlation between rainfall and landslides. The representation of landslides in the rainfall map is depicted in (Fig.8k) and has been categorized into 4 classes: 1600, 1800, 2000, and 2500 mm. The rainfall class of 1600 mm has a high weight contrast correlation with landslide.

Distance from road

In Nepal, roadside slopes are susceptible to small to medium-sized landslides with an average daily rainfall of 200 to 240 mm (Dahal et al. 2006). The excavation activities involved in road construction disrupt the natural slopes, elevating the potential for landslides. Along the highway, the slope close to the toe becomes weaker (Siddique et al., 2017). Landslides are frequently seen around road cuts. The primary cause of this is that the construction of a road degrades the slope's natural state. Furthermore, the road cutting exposes the joints and fractures that contribute to slope failures. Road construction frequently disrupts the slope and accelerates weathering, increasing the chances of a landslide happening. The current assessment used the distance from the road as a causal component of landslides. The distance from the road map has been divided into 6 different categories, which include: <100 m, 100-200 m, 200-300 m, 300-400 m, 400-500 m and >500 m (Fig. 8l). It shows that distance <100 m has a high positive weight contrast, while distances >500 m has a high negative contrast correlation with landslide. This elucidates that the slope near to road has more probability of slope failures.

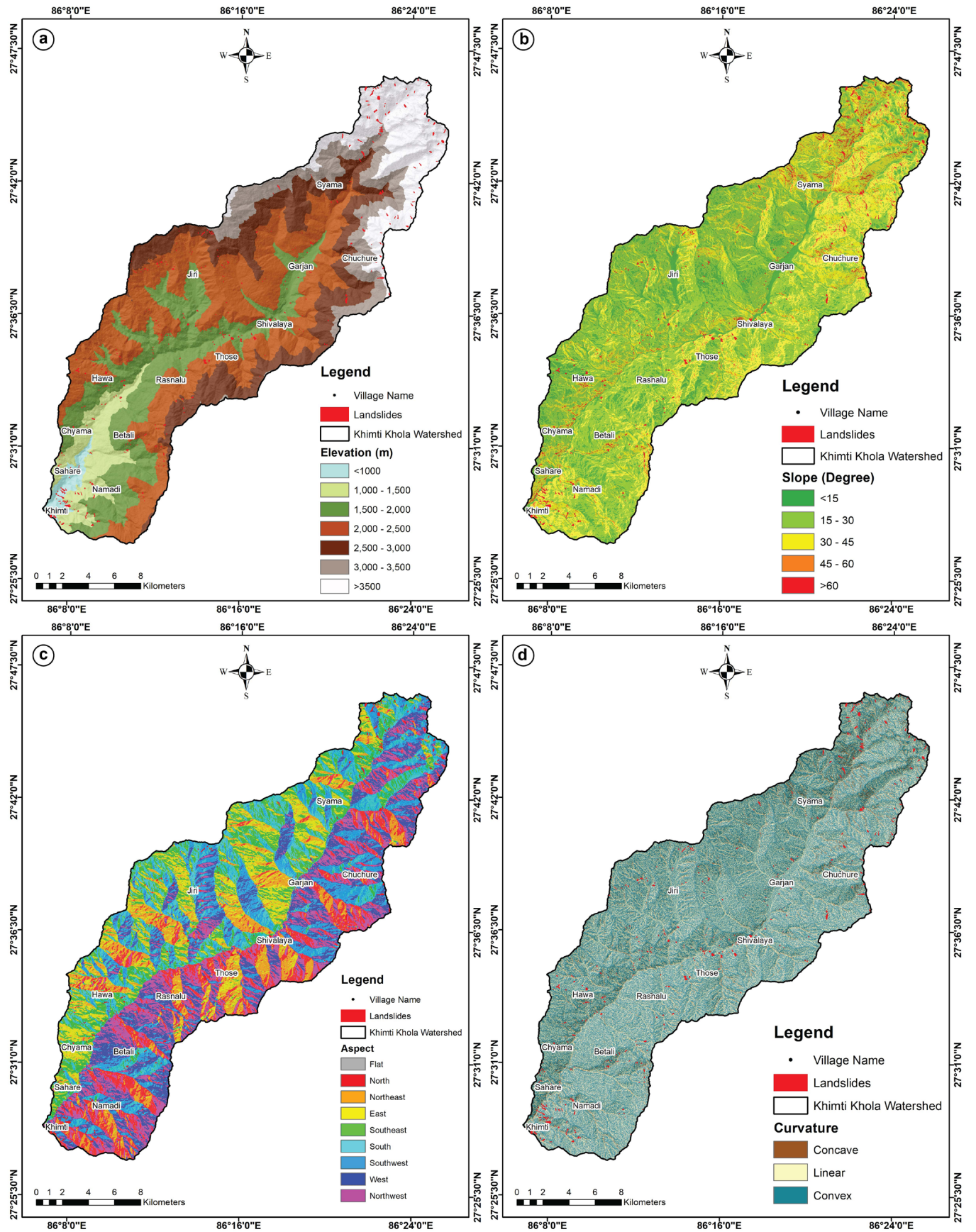


Fig. 6: Conditioning landslide factor maps of the study area: (a) Elevation; (b) Slope; (c) Aspect, (d) Curvature.

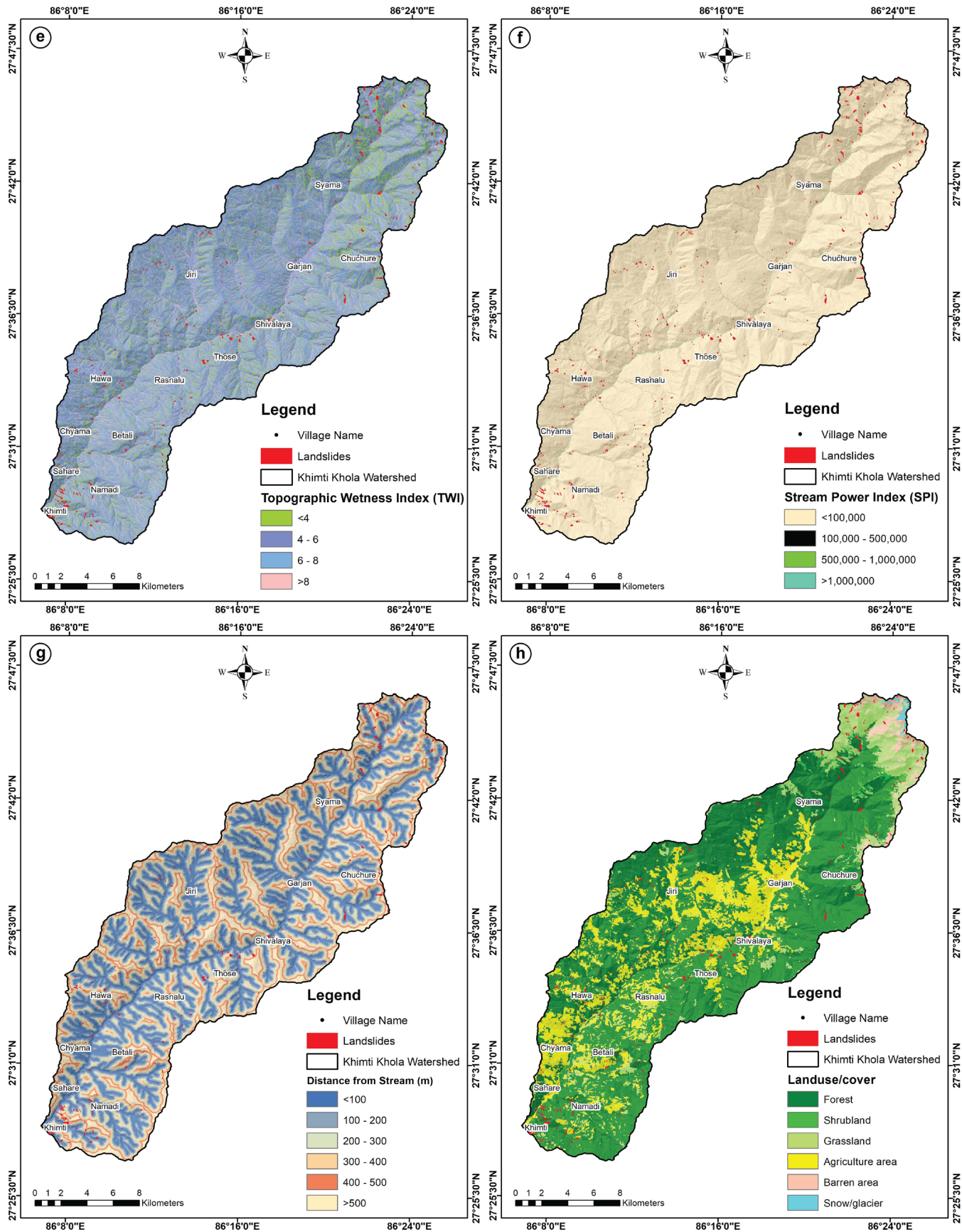


Fig. 7: Conditioning landslide factor maps of the study area: (e) TWI; (f) SPI; (g) Distance from stream (h) Landuse/cover.

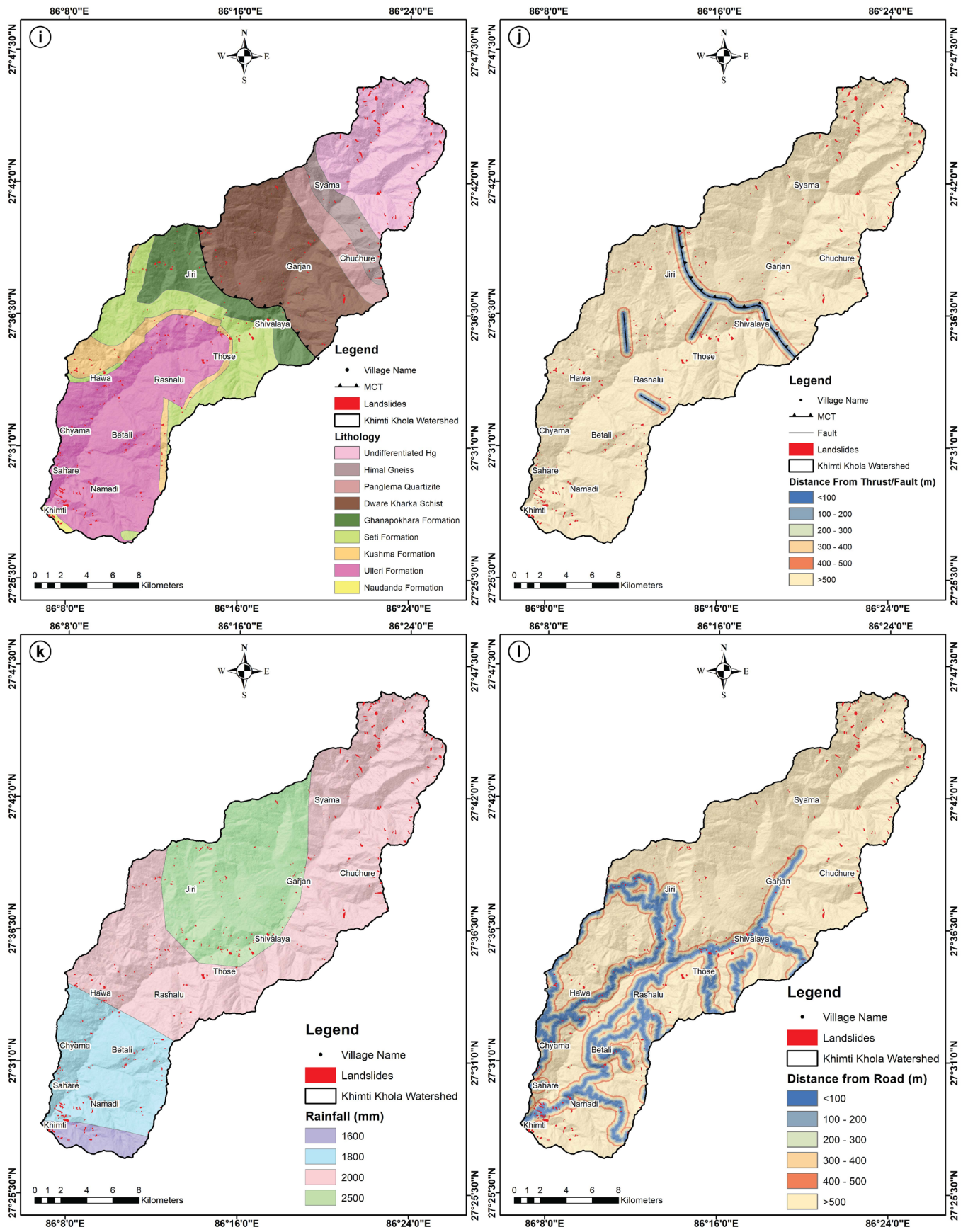


Fig.8: Landslide conditioning factor maps of the study area: (i) Lithology; (j) Distance from thrust/fault; (k) Rainfall, (l) Distance

Table 1: Weight values, variances, and standardized contrasts obtained from the Weights-of-Evidence method for all landslide conditioning factors.

Factors	Class	Class Pixel Count	Landslide Pixel Count	W ⁺	W ⁻	C	S ² (W ⁺)	S ² (W ⁻)	S(C)	C/S(C)
Elevation (m)	<1000	45137	868	1.623	-0.067	1.69	0.00115	2.26E-05	0.034	49.29
	1000 - 1500	183823	1186	0.518	-0.048	0.57	0.00084	5.48E-06	0.029	19.40
	1500 - 2000	573510	1846	-0.181	0.041	-0.22	0.00054	1.75E-06	0.023	-9.52
	2000 - 2500	952199	2089	-0.565	0.196	-0.76	0.00048	1.05E-06	0.022	-34.78
	2500 - 3000	479347	1133	-0.491	0.076	-0.57	0.00088	2.09E-06	0.030	-19.04
	3000 - 3500	266202	768	-0.291	0.026	-0.32	0.00130	3.77E-06	0.036	-8.76
	>3500	351863	3105	0.833	-0.201	1.03	0.00032	2.87E-06	0.018	57.36
Slope (Degree)	<15	357721	620	-0.805	0.077	-0.88	0.00161	2.8E-06	0.040	-21.93
	15-30	1497721	3581	-0.482	0.356	-0.84	0.00028	6.69E-07	0.017	-50.09
	30-45	876484	5524	0.491	-0.331	0.82	0.00018	1.15E-06	0.013	60.86
	45-60	105155	1178	1.071	-0.076	1.15	0.00085	9.62E-06	0.029	39.15
	>60	6199	92	1.356	-0.006	1.36	0.01087	0.000164	0.105	12.97
Aspect	Flat	0	0	0	0	0	0	0	0	0
	North	310143	920	-0.266	0.028	-0.29	0.00109	3.23E-06	0.033	-8.91
	Northeast	282192	688	-0.463	0.040	-0.50	0.00145	3.55E-06	0.038	-13.17
	East	308042	773	-0.434	0.042	-0.48	0.00129	3.25E-06	0.036	-13.21
	Southeast	353727	1266	-0.078	0.011	-0.09	0.00079	2.84E-06	0.028	-3.13
	South	351858	1947	0.360	-0.063	0.42	0.00051	2.86E-06	0.023	18.61
	Southwest	413861	2431	0.420	-0.093	0.51	0.00041	2.43E-06	0.020	25.22
	West	435471	1738	0.032	-0.006	0.04	0.00058	2.31E-06	0.024	1.56
	Northwest	387986	1232	-0.198	0.028	-0.23	0.00081	2.59E-06	0.029	-7.91
Curvature	Concave	150969	1352	0.848	-0.077	0.93	0.00074	6.68E-06	0.027	33.86
	Linear	993436	4172	0.086	-0.049	0.14	0.00024	1.01E-06	0.016	8.71
	Convex	1707676	5471	-0.186	0.226	-0.41	0.00018	5.87E-07	0.014	-30.39
Topographic Wetness Index (TWI)	<4	477245	1916	0.038	-0.008	0.05	0.00052	2.1E-06	0.023	1.98
	4 - 6	1552839	5791	-0.036	0.042	-0.08	0.00017	6.46E-07	0.013	-5.96
	6 - 8	608796	2413	0.025	-0.007	0.03	0.00041	1.65E-06	0.020	1.55
	>8	204400	875	0.102	-0.008	0.11	0.00114	4.91E-06	0.034	3.26
Stream Power Index (SPI)	<100000	2835384	10934	-0.003	0.696	-0.70	0.00009	3.54E-07	0.010	-72.92
	100000 - 500000	4804	48	0.955	-0.003	0.96	0.02083	0.00021	0.145	6.60
	500000 - 1000000	938	5	0.322	0.000	0.32	0.20000	0.001072	0.448	0.72
	>1000000	2154	8	-0.041	0.000	-0.04	0.12500	0.000466	0.354	-0.11
Distance from stream (m)	<100	816596	3998	0.240	-0.115	0.36	0.00025	1.23E-06	0.016	22.40
	100-200	645524	2391	-0.040	0.011	-0.05	0.00042	1.55E-06	0.020	-2.52
	200-300	496936	1933	0.009	-0.002	0.01	0.00052	2.02E-06	0.023	0.48
	300-400	385296	1371	-0.080	0.012	-0.09	0.00073	2.6E-06	0.027	-3.42
	400-500	268140	614	-0.522	0.041	-0.56	0.00163	3.74E-06	0.040	-13.96
	>500	239612	688	-0.296	0.023	-0.32	0.00145	4.19E-06	0.038	-8.35

Factors	Class	Class Pixel Count	Landslide Pixel Count	W ⁺	W ⁻	C	S ² (W ⁺)	S ² (W ⁻)	S(C)	C/S(C)
Landuse/Cover	Forest	1933277	6090	-0.203	0.327	-0.53	0.00016	5.19E-07	0.013	-41.25
	Shrubland	30366	350	1.103	-0.022	1.12	0.00286	3.33E-05	0.054	20.92
	Grassland	288186	2047	0.614	-0.100	0.71	0.00049	3.49E-06	0.022	32.21
	Agriculture area	544536	1727	-0.196	0.041	-0.24	0.00058	1.84E-06	0.024	-9.83
	Barren area	48663	725	1.363	-0.051	1.41	0.00138	2.09E-05	0.037	37.80
	Snow/Glacier	7308	56	0.691	-0.003	0.69	0.01786	0.000138	0.134	5.17
Lithology	Undifferentiated Hg	470362	3520	0.667	-0.206	0.87	0.00028	2.14E-06	0.017	51.62
	Himal Gneiss	111649	576	0.293	-0.014	0.31	0.00174	9E-06	0.042	7.34
	Panglerna Quartzite	129332	109	-1.523	0.037	-1.56	0.00917	7.74E-06	0.096	-16.28
	Dwara Kharka Schist	589043	1068	-0.756	0.130	-0.89	0.00094	1.7E-06	0.031	-28.93
	Ghanapokhara Formation	241673	423	-0.792	0.050	-0.84	0.00236	4.15E-06	0.049	-17.29
	Seti Formation	339198	805	-0.487	0.051	-0.54	0.00124	2.96E-06	0.035	-15.23
	Kushma Formation	818512	3191	0.011	-0.005	0.02	0.00031	1.23E-06	0.018	0.89
	Ulleri Formation	142961	834	0.416	-0.028	0.44	0.00120	7.04E-06	0.035	12.78
	Naudanda Formation	9394	469	0.240	-0.021	0.261	0.00213	0.000112	0.047	5.51
Distance from Thrust/ Faul (m)	<100	31752	45	-1.003	0.007	-1.01	0.02222	3.15E-05	0.149	-6.77
	100-200	31924	111	-0.104	0.001	-0.10	0.00901	3.14E-05	0.095	-1.10
	200-300	31828	81	-0.417	0.004	-0.42	0.01235	3.15E-05	0.111	-3.78
	300-400	33788	63	-0.728	0.006	-0.73	0.01587	2.97E-05	0.126	-5.82
	400-500	34588	45	-1.089	0.008	-1.10	0.02222	2.89E-05	0.149	-7.35
	>500	2688276	10650	0.027	-0.607	0.63	0.00009	3.73E-07	0.010	65.31
Rainfall (mm)	1600	84817	878	0.994	-0.053	1.05	0.00114	1.19E-05	0.034	30.88
	1800	495412	1968	0.030	-0.006	0.04	0.00051	2.03E-06	0.023	1.62
	2000	1552195	6311	0.053	-0.068	0.12	0.00016	6.47E-07	0.013	9.61
	2500	719700	1838	-0.413	0.108	-0.52	0.00054	1.39E-06	0.023	-22.33
Distance from Road (m)	<100	236524	1711	0.633	-0.083	0.72	0.00058	4.26E-06	0.024	29.50
	100-200	178936	612	-0.120	0.008	-0.13	0.00163	5.61E-06	0.040	-3.15
	200-300	154072	441	-0.299	0.015	-0.31	0.00227	6.51E-06	0.048	-6.57
	300-400	146528	557	-0.014	0.001	-0.01	0.00180	6.85E-06	0.042	-0.35
	400-500	131268	448	-0.122	0.006	-0.13	0.00223	7.64E-06	0.047	-2.70
	>500	2004776	7226	-0.067	0.144	-0.21	0.00014	5.01E-07	0.012	-17.92

RESULT AND DISCUSSION

Landslide Susceptibility Map

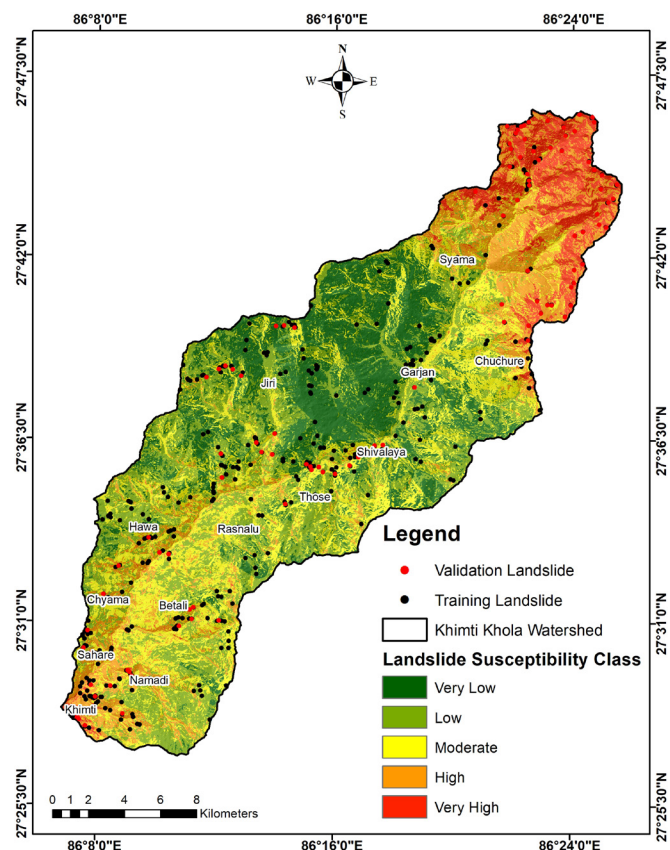


Fig. 9: Susceptibility map of study area landslide

A total of 12 factors influencing landslides were considered for the susceptibility assessment. In this assessment, we can see that the highest positive weight contrast was found in the >3500 m elevation zone. In the case of slope, evidently, the slope angle of 30 - 45 degree has high weight contrast. The aspect map shows a significant weight contrast link between landslides and the southwest-facing slope. The curvature map reveals that the concave has high weight contrast. The distance from the stream map shows that distances <100 m has a high positive weight contrast, while distances 400-500 m has a

high negative contrast correlation with landslide. It shows that while the frequency of landslides increases close to streams, it drastically lowers as one gets farther away from them. The barren area and following grassland have the highest weight contrast correlation with landslides. In lithology, the highest weight contrast is in the Undifferentiated Hg and following the Ulleri Formation. Notably, the Main Central Thrust (MCT) passes in close proximity to the meeting point of Yelun Khola and Khimti Khola in the Shivalaya area. Ekamphedi landslide in the Shivalaya area has been found to have a strong correlation with the MCT. There is a strong weight contrast link between landslides and the 1600 mm rainfall class. Regarding the distance from the road map, it demonstrates that they are more likely to occur at distances less than 100 meters and more frequently at distances greater than 500 meters. This elucidates that the slope near to road has more probability of slope failures.

Following the Weights of evidence (WoE) approach in ArcGIS, on the basis of the location of all landslides, the susceptibility map of landslide is created. Using the natural breaks method, this map

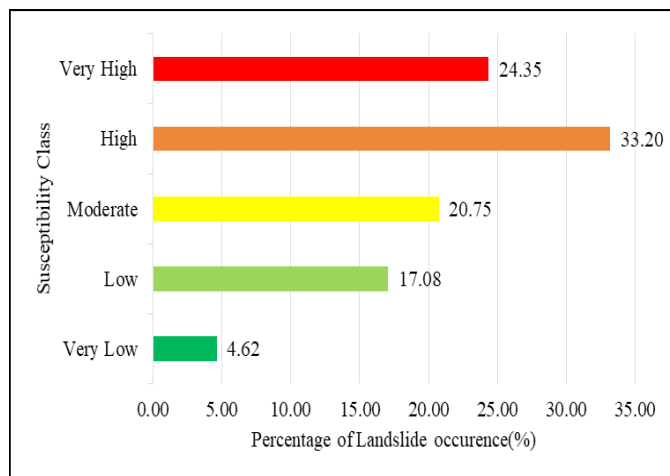


Fig. 10: Landslide distribution at different susceptibility classes of landslide

Table 2: Susceptible zones and the details of landslide density on the basis of the Weights-of-Evidence (WoE) method.

Susceptible Zone	Class Area		Landslide Area		Landslide density
	Value (m ²)	Percentage (%)	Value (m ²)	Percentage (%)	
Very Low	92265468.75	20.78	79218.75	4.62	0.09
Low	134283906.3	30.24	292968.75	17.08	0.22
Moderate	112054687.5	25.23	355781.25	20.75	0.32
High	73866250	16.63	569375	33.20	0.77
Very High	31637968.75	7.12	417500	24.35	1.32

is classified into 5 categories as Very High, High, Moderate, Low, Very Low (Fig.9). The detailed results are summarized in Table 2, with each class covering 7.12%, 16.63%, 25.23%, 30.24%, and 20.78% of the total area of the Khimti Khola watershed, respectively. The landslide density is 1.32% in the Very High susceptibility zone and 0.09% in the Very Low susceptibility zone, respectively.

The findings show that the Khimti Khola watershed experiences a 33.2% landslide occurrence percentage in the High susceptibility zone of the total area. Additionally, the Very Low, Low, Moderate and the Very High susceptibility zones cover 4.62%, 17.08%, 20.75% and 24.35% landslide occurrences, respectively (Fig.10).

6.2 Validation of the Model

In this assessment, the model is validated using the Area Under Curve (AUC). The region between the horizontal axis and specific curve that depicts changes in the classification results is known as the AUC curve. The Area Under Curve (AUC) is used in this assessment for the validation of the model. ArcSDM, a tool for ROC analysis of spatial models for GIS, is used to create the graph (Mas J-F et al., 2013) and plotted using a reclassified landslide susceptibility map for both training and validating data sets, producing false positive rate (FPR) and true positive rate curves respectively.

The assessment identified a total of 415 landslides in the Khimti Khola watershed, through which 75% of landslides i.e. 311 were selected as training data to build the landslide susceptibility map and the remaining 25 % i.e. 104 landslides were used for validation. The AUC for the landslide susceptibility map is 0.83, 83% (Fig.11), the results demonstrate a very good degree of accuracy and satisfaction.

CONCLUSIONS

The landslide susceptibility assessment was conducted in the Khimti Khola Watershed with an area of 440 km². Within the study area, the assessment identified 415 landslides, encompassing an area of 1.715 Km², equivalent to 0.39% of the total study area. The majority of landslides occurred at high elevations, steep slopes, areas with high precipitation, and areas with low vegetation cover. The high-resolution terrain- corrected ALOS PALSAR DEM; 12.5 meters by 12.5 meters per pixel resolutions. is utilized for the present assessment. Using the Weights of evidence (WoE) technique, the study concluded the susceptibility map from selected conditioning factors classes processed in ArcGIS and in 5 classes, the map was categorized as: Very High, High, Moderate, Low and Very Low. Each class covers 7.12%, 16.63%, 25.23%, 30.24%, and 20.78% of the total study area, respectively.

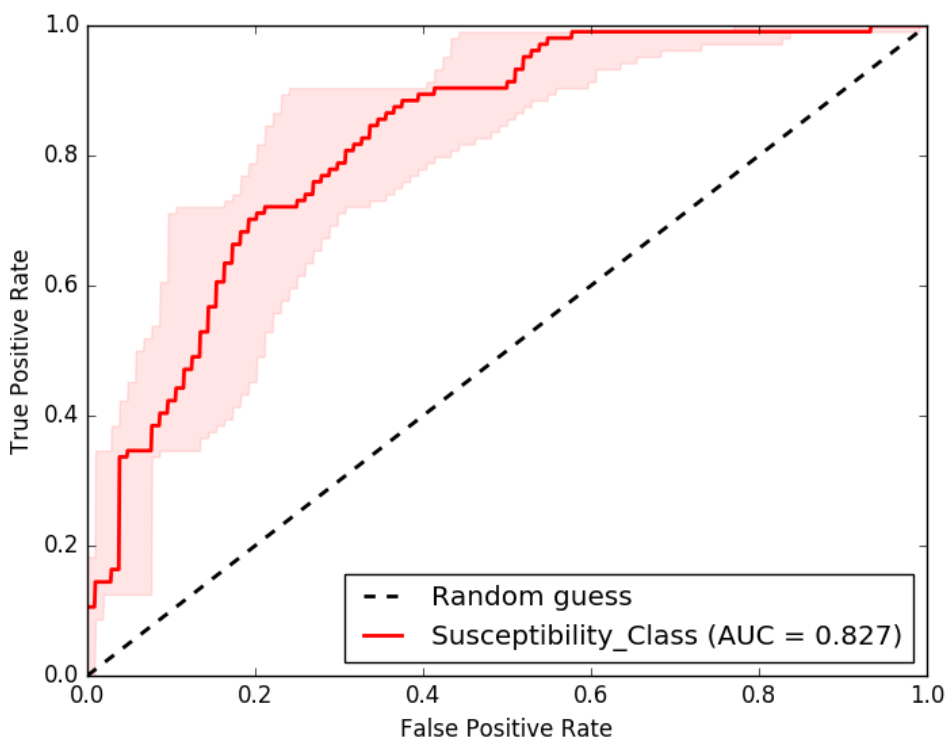


Fig. 11: Area under curve (AUC).

According to the findings, the high susceptibility zone contains 33.2% of landslide occurrence out of the total area in the Khimti Khola watershed. Similarly, 24.35%, 20.75%, 17.08% and 4.62 % landslide occurrence is there in the very high, moderate, low and very low landslide susceptibility zone. Landslide density in the very high susceptible zone is 1.32%, gradually diminishing towards the zone with very low susceptibility, where it is 0.09%. The results of this assessment can be used as a reference for future research in other regions with similar characteristics. In this assessment, the model is validated using Area Under Curve (AUC) and graphically represented using ArcSDM. In the Khimti Khola watershed, total 415 landslides were recognized. Among these, 75% of landslides i.e. 311 were utilized for susceptibility mapping, and the remaining 25% i.e. 104 landslides were employed for model validating. The AUC for the landslide susceptibility map is 83%, indicating a very good degree of accuracy and satisfaction.

The resulting susceptibility map provides information on predicting areas prone to landslides, thus making it a vital tool for disaster preparedness, future construction planning and development projects. It is recommended that the map be utilized to avoid high susceptibility zones during project implementation, to minimize the risk of potential landslides, and to ensure the sustainability of all involved.

ACKNOWLEDGEMENTS

The authors express extreme gratitude to the the Central Department of Geology, Tribhuvan University as well as all the reviewers for their important time and recommendations to improve the manuscript.

REFERENCES

- Alaska Satellite Facility. Available online <https://asf.alaska.edu>.
- Batar, A.K. and Watanabe, T., 2021. Landslide susceptibility mapping and assessment using geospatial platforms and weights of evidence (WoE) method in the Indian Himalayan region: Recent developments, gaps, and future directions. *ISPRS Int. Jour. Geo-Info.*, v. 10(3), ar 114. <https://doi.org/10.3390/ijgi10030114>.
- Beven, K.J. and Kirkby, M.J., 1979. A physically based, variable contributing area model of basin hydrology, *Hydro. Sci. Jour.*, v. 24(1), pp. 43–69. <https://doi.org/10.1080/02626667909491834>.
- Bonham-Carter, G.F., 1989. Weights of evidence modelling: a new approach to mapping mineral potential. In: *Statistical applications in the earth sciences*, pp.171-183.
- Cao, Y., Wei, X., Fan, W., Nan, Y., Xiong, W., and Zhang, S., 2021. Landslide susceptibility assessment using the weight of evidence method: A case study in Xunyang area, China. *PLoS One*, v. 16, pp. 1-18. <https://doi.org/10.1371/journal.pone.0245668>.
- Chimidi, G., Raghuvanshi, T.K., Suryabhadgavan K.V., 2017. Landslide hazard evaluation and zonation in and around Gimbi town, western Ethiopia – a GIS-based statistical approach. *Appl. Geomat.*, v. 9(4), pp. 219–236. <https://doi.org/10.1007/s12518-017-0195-x>.
- Dahal, R.K., Hasegawa, S., Nonomura, A., Yamanaka, M., Dhakal, S., Paudyal, P., 2008. Predictive modelling of rainfall-induced landslide hazard in the Lesser Himalaya of Nepal based on weights-of-evidence. *Geomorphology*, v. 102, pp. 496–510. <https://doi.org/10.1016/j.geomorph.2008.05.041>.
- Dahal, R.K. and Hasegawa, S., 2008. Representative rainfall thresholds for landslides in the Nepal Himalaya. *Geomorphology*, v. 100(3-4), pp. 429-443. <https://doi.org/10.1016/j.geomorph.2008.01.014>.
- Dahal, R.K., Hasegawa, S., Masuda, T. and Yamanaka, M., 2006. Roadside slope failures in Nepal during torrential rainfall and their mitigation. *Disaster mitigation of debris flows, slope failures and landslides*. Universal Academy Press, Inc. / Tokyo, Japan, pp. 503-514.
- Dahal, R.K., Hasegawa, S., Nonomura, A., Yamanaka, M., Masuda, T. and Nishino, K., 2008. GIS-based weights-of-evidence modelling of rainfall-induced landslides in small catchments for landslide susceptibility mapping. *Envi. Geol.*, v. 54, pp. 311-324. <https://doi.org/10.1007/s00254-007-0818-3>.
- Dai, F.C., Lee, C.F. and Ngai, Y.Y., 2002. Landslide risk assessment and management: an overview. *Engi. Geol.*, v. 64(1), pp. 65-87. [https://doi.org/10.1016/S0013-7952\(01\)00093-X](https://doi.org/10.1016/S0013-7952(01)00093-X).
- Dam, N.D., Amiri, M., Al-Ansari, N., Prakash, I., Le, H.V., Nguyen, H.B.T. and Pham, B.T.,

2022. Evaluation of shannon entropy and weights of evidence models in landslide susceptibility mapping for the Pithoragarh district of Uttarakhand State, India. *Advances in Civil Engineering*, v. 2022, pp. 1-16, <https://doi.org/10.1155/2022/6645007>.
- Devkota, K.C., Regmi, A.D., Pourghasemi, H.R., Yoshida, K., Pradhan, B., Ryu, I.C., Dhital, M.R. and Althuwaynee, O.F., 2013. Landslide susceptibility mapping using certainty factor, index of entropy and logistic regression models in GIS and their comparison at Mugling–Narayanghat road section in Nepal Himalaya. *Nat. Hazards*, v. 65(1), pp. 135–165. <https://doi.org/10.1007/s11069-012-0347-6>.
- Ercanoglu, M., and Gokceoglu, C., 2004. Use of fuzzy relations to produce landslide susceptibility map of a landslide prone area (West Black Sea Region, Turkey). *Engi. Geol.*, v. 75, pp. 229-250. <https://doi.org/10.1016/j.enggeo.2004.06.001>.
- Gadtaula, A., Dhakal, S., 2019. Landslide susceptibility mapping using weight of evidence method in Haku, Rasuwa district, Nepal. *Jour. Nepal Geol. Soc.*, v. 58, pp. 163-171. <https://doi.org/10.3126/jngs.v58i0.24601>.
- Ghimire, M., 2011. Landslide occurrence and its relation with terrain factors in the Siwalik Hills, Nepal: Case study of susceptibility assessment in three basins. *Nat. Hazards*, v. 56, pp. 299–320. <https://doi.org/10.1007/s11069-010-9569-7>.
- Girma, F., Raghuvanshi, T.K., Ayenew, T., Hailemariam, T., 2015. Landslide hazard zonation in Ada Berga district, Central Ethiopia – a GIS based statistical approach. *Jour. Geom.*, v. 9(1), pp. 25–38.
- Guzzetti, F., 2005. Landslide Hazard and Risk Assessment. PhD Thesis. Mathematics-Scientific Faculty, University of Bonn, Bonn, Germany. 389 p.
- ICIMOD., 2013. Land cover of Nepal 2010 [Data set]. ICIMOD. <https://doi.org/10.26066/rds.9224>.
- Kavzoglu, T., Sahin, E.K. and Colkesen, I., 2015. An assessment of multivariate and bivariate approaches in landslide susceptibility mapping: a case study of Duzkoy district. *Nat. Hazards*, v. 76(1), pp. 471–496. <https://doi.org/10.1007/s11069-014-1506-8>.
- Kayastha, P., Dhital, M.R., De Smedt, F., 2012. Landslide susceptibility mapping using the weight of evidence method in the Tinau watershed, Nepal. *Nat. Hazards*, v. 63, pp. 479–498. <https://doi.org/10.1007/s11069-012-0163-z>.
- KC, D., Dangi, H., Hu, L., 2022. Assessing Landslide Susceptibility in the Northern Stretch of Arun Tectonic Window, Nepal. *Civil Eng.*, v. 3(2), pp. 525–540. <https://doi.org/10.3390/civileng3020031>.
- Lee, S. and Choi, J., 2004. Landslide susceptibility mapping using GIS and the weight-of-evidence model. *Int. Jour. Geogra. Infor. Sci.*, v. 18(8), pp. 789–814. <https://doi.org/10.1080/13658810410001702003>.
- Mandal, B., Mondal, S. and Mandal, S., 2023. GIS-based landslide susceptibility zonation (LSZ) mapping of Darjeeling Himalaya, India using weights of evidence (WoE) model. *Arab. Jour. Geosci.*, v. 16, ar. 421. <https://doi.org/10.1007/s12517-023-11523-w>.
- Mas, J-F., Soares Filho, B., Pontius, R.G., Farfán Gutiérrez, M., Rodrigues, H., 2013. A Suite of Tools for ROC Analysis of Spatial Models. *ISPRS Int. Jour. Geo-Info.*, v. 2(3), pp. 869-887. <https://doi.org/10.3390/ijgi2030869>
- Mohammady, M., Pourghasemi, H.R., Pradhan, B., 2012. Landslide susceptibility mapping at Golestan Province, Iran: a comparison between frequency ratio, Dempster–Shafer, and weights-of-evidence models. *Jour. Asian Eart. Sci.*, v. 61, pp. 221–36. <https://doi.org/10.1016/j.jseaes.2012.10.005>.
- Moore, I.D. and Grayson, R.B., 1991. Terrain-based catchment partitioning and runoff prediction using vector elevation data, *Wat. Reso. Res.*, v. 27(6), pp. 1177-1191. <https://doi.org/10.1029/91WR00090>.
- Neuhäuser, B. and Terhorst, B., 2007. Landslide susceptibility assessment using “weights-of-evidence” applied to a study area at the Jurassic escarpment (SW-Germany). *Geomorphology*, v. 86(1-2), pp.12-24. <https://doi.org/10.1016/j.geomorph.2006.08.002>
- Pachauri, A.K. and Pant, M., 1992. Landslide hazard mapping based on geological attributes, *Engi. Geol.*, v. 32, pp. 81–100. [https://doi.org/10.1016/0013-7952\(92\)90020-Y](https://doi.org/10.1016/0013-7952(92)90020-Y).

- Pradhan, B. and Lee, S., 2010. Landslide susceptibility assessment and factor effect analysis: backpropagation artificial neural networks and their comparison with frequency ratio and bivariate logistic regression modelling. *Envi. Mod. and Soft.*, v. 25(6), pp. 747–759. <https://doi.org/10.1016/j.envsoft.2009.10.016>.
- Pradhan, B., 2010. Landslide susceptibility mapping of a catchment area using frequency ratio, fuzzy logic and multivariate logistic regression approaches. *Jour. Indian Soc. of Rem. Sen.*, v. 38, pp. 301-320. <https://doi.org/10.1007/s12524-010-0020-z>.
- Regmi, A.D., Devkota, K.C., Yoshida, K., Pradhan, B., Pourghasemi, H. R., Kumamoto, T. and Akgun, A., 2014a. Application of frequency ratio, statistical index, and weights-of-evidence models and their comparison in landslide susceptibility mapping in central Nepal Himalaya, *Arab. Jour. Geosci.* v. 7(2), pp. 725–742. <https://doi.org/10.1007/s12517-012-0807-z>
- Regmi, A.D., Yoshida, K., Pourghasemi, H.R., Dhital, M.R. and Pradhan, B., 2014b. Landslide susceptibility mapping along bhalubang-shiwapur area of mid-western Nepal using frequency ratio and conditional probability models, *Jour. Moun. Sci.*, v. 11(5), pp. 1266–1285. <https://doi.org/10.1007/s11629-013-2847-6>.
- Shrestha, S.B., Shrestha, J.N. and Sharma, S.R., 1984. Geological Map of Eastern Nepal, 1:250000. Ministry of Industry, Department of Mines and Geology, Lainchaur, Kathmandu.
- Siddique, T., Pradhan, S.P., Vishal, V., Mondal, M.E., Singh, T.N., 2017. Stability assessment of Himalayan road cut slopes along National Highway 58, India. *Envi. Ear. Sci.*, v. 76, ar. 759. <https://doi.org/10.1007/s12665-017-7091-x>.
- Thakurathi, R., Maharjan, S., Ghimire, B.J. and Pandey, V.P., 2021. Landslide Susceptibility Mapping of Khimti Watershed, Nepal. *Nepal Jour. of Civ. Engi.*, v. 2(1), pp. 37-48.
- Upreti, B.N., 2001, Physiography and Geology of Nepal and their bearing on the landslide problem. In: *Landslide hazard mitigation in the Hindu Kush-Himalayas*, Tianchi L., Chalise, S.R. and Upreti, B.N. (eds.), ICIMOD publication, pp. 31–49.
- van Westen, C.J., 1993. Application of geographic information systems to landslide hazard zonation. [PhD Thesis - Research external, graduation external, Delft University of Technology]. International Institute for Geo-Information Science and Earth Observation. 245 p. Available online <http://resolver.tudelft.nl/uuid:a59d2eca-ab58-41e6-91c9-01e4e090cf81>.
- van Westen, C.J., Soeters, R. and Sijmons, K., 2000. Digital geomorphological landslide hazard mapping of the Alpage area, Italy. *Int. Jour. of Appl. Earth Obs. and Geoinfo.*, v. 2(1), pp.51-60. [https://doi.org/10.1016/S0303-2434\(00\)85026-6](https://doi.org/10.1016/S0303-2434(00)85026-6).